PHYSICAL REVIEW B **66**, 054304 (2002)

Restricted dynamics of a supercooled liquid in a polymer matrix

C. Svanberg,[1,*] R. Bergman,[1] P. Jacobsson,[1] and L. Börjesson[2]
[1]*Department of Experimental Physics, Chalmers University of Technology, SE-412 96 Göteborg, Sweden*
[2]*Department of Applied Physics, Chalmers University of Technology, SE-412 96 Göteborg, Sweden*

(Received 4 September 2001; revised manuscript received 12 February 2002; published 29 August 2002)

We have performed dielectric spectroscopy on polymer gels consisting of propylene carbonate (PC) mixed with a polymer, poly(methyl methacrylate) (PMMA). The compositions of the investigated systems range from pure PC via PC/PMMA mixtures to pure polymer. In the supercooled regime of all the mixed compositions a dielectric loss peak, attributed to the main α relaxation of PC, is observed. The main influence of the restriction on the dynamics of PC by the polymer matrix is an increasingly slower and broader α relaxation for higher polymer concentrations. We show that there are strong correlations between the shape of the relaxation function, the structural relaxation time, and the macroscopic viscosity. Large polymer-induced changes at the low-frequency side of the loss peak coincide with a moderate increase in the relaxation time and are attributed to spatial restriction imposed by the polymer on long-range motion of PC. Changes at the high-frequency side of the loss peak are shown to correlate with a dramatic increase of the relaxation time, which is attributed to a gradual increase of the number of PC molecules that are affected by the polymer. Furthermore, the temperature and polymer concentration dependencies of the shape and strength of the loss peak can quantitatively be explained by cooperativity effects of the dynamics in the supercooled solvent.

DOI: 10.1103/PhysRevB.66.054304 PACS number(s): 64.70.Pf, 77.22.Gm

I. INTRODUCTION

The dynamics of polymer gels and solutions is presently attracting a lot of scientific attention, boosted by the attempts to model the behavior.[1,2] Most studies concern the diffusional properties of the solvent and the polymer at temperatures well above the supercooled regime. This study focuses instead on the relaxational behavior of the solvent in the gel close to the glass transition temperature. In the vicinity of the glass transition temperature the dynamics of supercooled liquids is believed to be dominated by cooperative motions[3–6] and the length scales of such motions have been suggested to be in the range 1–10 nm.[7–13] This motivates investigations of confined systems of the order of nanometers, where the spatial dimension is of the same order as the cooperative length scale, in order to examine a length scale dependence of the dynamics in supercooled liquids.[11–21] However, in experiments on glass formers confined to small geometries the finite-size effects of the glass transition can be obscured by structural and/or surface effects, e.g., as discussed by Pelster.[22] Therefore, experiments using various geometries to achieve the spatial restrictions will provide vital information. Experimentally, spatial restriction has most frequently been obtained by confining the glass former in a porous glass.[12–18] In this paper an alternative way to introduce restriction of the dynamics is adopted, i.e., to dissolve a polymer into a glass forming liquid, such that a polymer gel is created where the slower polymer matrix imposes spatial restrictions on the liquid molecules. Thus the dynamics of the solvent in gels is confined, if by confinement we mean that the solvent molecules are not free to move to any position as it might be occupied by the, on the time scale of the solvent dynamics, static polymer matrix. In this paper we will show that our experimental results for the polymer gels can be interpreted using the concepts commonly employed when discussing confinement effects. In addition, polymer gels have the appealing property that the concentration of the polymer, which restricts the molecular motion of the solvent, is easy to control and to vary over a wide range.

The polymer gel systems examined in the present study consist of a mixture of poly(methyl methacrylate) (PMMA) and propylene carbonate (PC). The two components are inherently different since PC is a low molecular glass forming liquid while PMMA is a polymeric glass former. According to Angell's classification[23] PC is a fragile glass former,[24] i.e., the viscosity and structural relaxation time change rapidly with temperature slightly above the glass transition temperature, $T_g^{\mathrm{PC}} \approx 160$ K. Syndiotactic PMMA is an essentially amorphous polymer and a fragile glass former.[24] The glass transition temperature for PMMA is much higher compared to PC, $T_g^{\mathrm{PMMA}} \approx 380$ K, and several relaxation processes have been observed.[25,26] PMMA and PC are miscible for all concentrations examined in this study. Thus, in this system the restrictions on the PC molecules can be systematically controlled by altering the PMMA content. The mixture of the two well-characterized glass formers provides an interesting model system for an examination of the glass transition dynamics of polymer gels.

Of specific interest in the present study is the evolution of the shape of the main structural relaxation, the so-called α relaxation of PC when spatially restricted by a polymer matrix. The α relaxation for bulk PC is well described by the empirical Kohlrausch-Williams-Watts (KWW) function,

$$\phi(t) = \phi_0 \exp[-(t/\tau_{\mathrm{KWW}})^{\beta_{\mathrm{KWW}}}], \tag{1}$$

where τ_{KWW} is a typical relaxation time and β_{KWW} the stretching parameter. Explaining the stretched exponential decay is one of the many challenges in any attempt to theoretically describe the liquid-glass transition. The stretching of the relaxation has been suggested to be due to dynamic heterogenities,[27,28] which may in turn be related to regions of

TABLE I. Concentrations for the investigated samples and the symbols used throughout this paper are shown. The VFT parameters obtained from the curve fits are also included.

Name	Symbol	PC (%)	PMMA (%)	T_0 (K)	D	$\log(\tau_0\,(\mathrm{s}))$
PC100	⊠	100.0	0.0	134.4	6.177	−13.5
PC90	⋈	89.9	10.1	134.2	6.388	−13.5
PC80	⧗	80.6	19.4	134.7	6.439	−13.5
PC75	▽	75.2	24.8	134.8	6.751	−13.5
PC70	○	69.6	30.4	135.3	6.591	−13.5
PC65	◿	65.4	34.6	135.1	6.661	−13.5
PC60	△	60.1	39.9	135.6	6.638	−13.5
PC55	◸	55.4	44.6	135.4	6.491	−13.24
PC50	□	50.4	49.6	137.3	6.120	−12.77
PC45	◺	45.0	55.0	141.2	5.912	−12.08
PC40	◇	38.8	61.2	141.4	5.833	−11.96
PC35	◹	35.1	64.9	143.9	5.687	−11.87
PC30	◇	30.1	69.9			
PMMA	⊗	0.0	100.0			

cooperativity, giving rise to a distribution of relaxation times. In most models of cooperative dynamics the regions of cooperativity become smaller with increasing temperature[3] and at some temperature sufficiently well above the glass transition temperature T_g, the cooperativity effects should be negligible. The α-relaxation dynamics would then approach an exponential time decay, i.e., a Debye frequency response. Experimentally, Schönhals *et al.*[29] showed that for bulk PC the shape of the relaxation function in fact exhibits a transition from KWW to a Debye relaxation at roughly 50 K above T_g. This transition also coincides with a transition from low-temperature Vogel-Fulcher-Tammann (VFT) behavior to a high-temperature Arrhenius behavior.[29] These findings suggest that a transition from cooperative to noncooperative motion occurs about 50 K above T_g for PC.

In this paper we present experiments performed on PC/PMMA gel systems over a wide range of temperatures, frequencies, and PC concentrations. We focus on the temperature and concentration dependencies of the relaxation time and shape of the α relaxation. We show that there are strong correlations between the macroscopic viscosity, the structural relaxation time, and the shape of the relaxation function. Furthermore, we discuss cooperative dynamical features of PC in bulk and when it is restricted to move within the polymer matrix.

II. EXPERIMENT

The compositions of the investigated samples range from pure PC via PC/PMMA mixtures to pure PMMA. Two PC/PMMA mixtures were used for a range of PC concentrations accomplished by controlled evaporation of PC at elevated temperatures. In total four samples were utilized to cover the whole concentration range: (i) pure PC, (ii) PMMA with 90% down to 70% PC, (iii) PMMA with 80% down to 30% PC, and (iv) pure PMMA. The percentages are consistently reported throughout this paper as weight percentages and the details of all the investigated samples are presented in Table I.

To produce the sample, polymer films were first prepared by dissolving high molecular weight PMMA ($M_W = 1\,220\,500$, $M_W/M_n = 1.39$, Polymer Source Inc.) in toluene. Thin polymer films were obtained by heating droplets of the PMMA/toluene solution to 393 K under vacuum for more than 12 h so that all the solvent evaporated. Sample iv (pure PMMA) was further treated at 413 K for 48 h under vacuum to minimize the amount of residual solvent in the sample. For the polymer gel samples, between two and five films with a total thickness of the order of 10 μm were stacked on a gold electrode and the weight of the polymer was determined. Propylene carbonate (Fluka) was added onto the films and the second electrode was placed on top. The samples were made with an excess of PC and equilibrated at 413 K before any measurements were performed. The evaporation of the solvent was monitored by weighing the sample until a chosen molar composition was obtained. This procedure yields transparent and colorless samples. The weight of the samples was also determined just before and after the dielectric experiments and the error in concentration could thus be estimated to be less than 1%. After the completed experiment with a given PC concentration, the samples were reused by heating them up to 413 K again and monitoring the solvent evaporation until the next chosen solvent concentration was obtained. In order to check whether the evaporation procedures alter the properties of the system, samples ii and iii were made with overlapping concentrations. In the overlapping region the two samples show identical response within experimental uncertainty. Additional characterization by Raman spectroscopy (Dilor Labram) was performed on samples produced under similar conditions. These experiments show that the adopted sample preparation procedure gives homogeneous polymer gels at length scales of the order of micrometers. Recent small-angle neutron-scattering (SANS) experiments reveal an inherent heterogeneity at lengths scales of the order of 200 Å possibly originating from static polymer concentration fluctuations due to crosslinks in the system.[30] The amplitude of the fluctuations

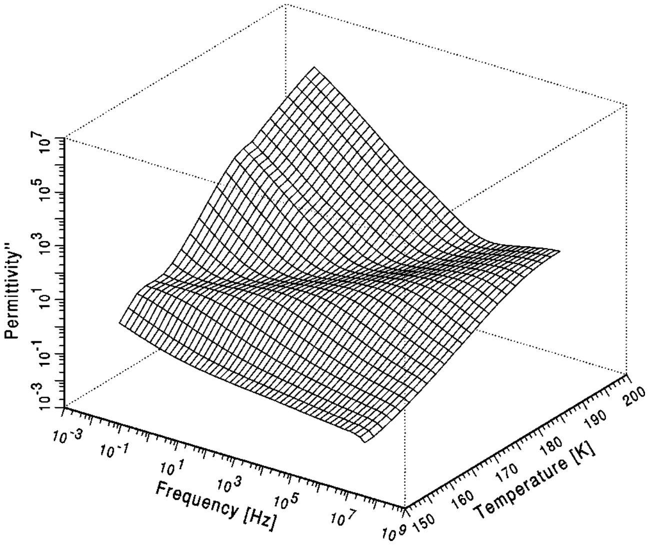

FIG. 1. Imaginary part of the permittivity ε'', obtained for a polymer gel consisting of 70% PC and 30% PMMA as a function of temperature and frequency.

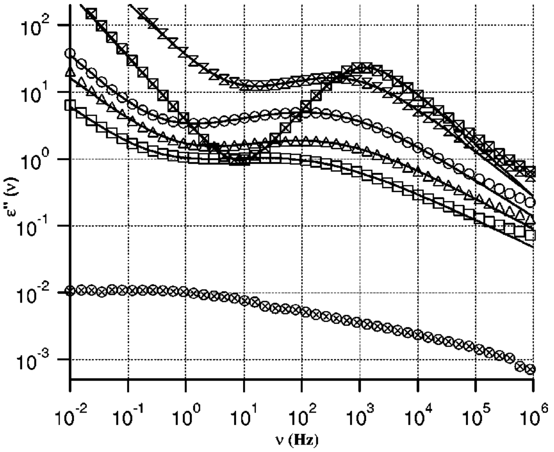

FIG. 2. Imaginary part of the permittivity ε'' versus frequency at $T = 172$ K for pure PC, PC/PMMA mixtures and pure PMMA. The symbols used for PC, PMMA, and the mixed systems are given in Table I.

is hard to estimate from the SANS experiments due to overlapping structural features. The recycling procedure of the samples may, however, produce a polymer concentration gradient towards the edge of the sample. From the Raman experiments we estimate that the macroscopic maximum deviation from the average concentration is less than 5%. We also performed complementary dielectric measurements at room temperature before and after the experiments. No detectable change in the response was revealed, and we can thus rule out any major geometrical changes of the sample.

The experiments were performed using a high-resolution dielectric spectrometer (Novocontrol, Alpha) over the frequency range from 10^{-2} to 10^{7} Hz. During the experiments the samples were placed in an airtight sample cell in order to minimize evaporation while collecting data. The temperature of the sample was controlled with a cryostat (Novocontrol) with an accuracy of ± 0.1 K. All experiments were initialized by fast cooling, roughly 10 K/min, down to 156 K, which is below T_g for pure PC. This procedure effectively decreased the probability of crystallization that is well documented for pure PC (Ref. 31) that has a melting temperature of $T_m = 218$ K. The isothermal measurements were performed at 2 K intervals, where each measurement lasted roughly 30 min.

III. RESULTS

The imaginary part of the dielectric response $\varepsilon''(\omega)$, for a polymer gel with 70% PC and 30% PMMA is shown in Fig. 1 over the temperature range 156–200 K. Two features are readily observed, a dispersion at low frequencies and a highly temperature-dependent loss peak at higher frequencies. To examine the origin of these features Fig. 2 shows $\varepsilon''(\omega)$ for different PC/PMMA ratios at a fixed temperature $T = 172$ K. The symbols used for the different concentrations are the same in all graphs in this paper and are shown in Table I. Our experimental data for pure PC are in excellent agreement with previous reports.[29,31] The dispersion observed at low frequencies can be described by a power law. However, it is not inversely proportional to the frequency, and can therefore not be directly attributed to normal conductivity. In the present experiments, the power-law exponent of the low-frequency dispersion tends to increase with temperature and PC concentration. The other directly observable feature in Figs. 1 and 2 is the loss peak, which for pure PC is the well-known α relaxation. The almost identical peak frequency and high-frequency shape of pure PC and the mixtures with a very high concentration of PC enables us to attribute the loss peak in the polymer/solvent mixtures to relaxation of dipoles in PC. This assignment is further supported by the observation that the dielectric response of the pure polymer is at least two orders-of-magnitude smaller and almost featureless (see Fig. 2) at these temperatures. This is consistent with the smaller dielectric constant for PMMA compared to PC. This also suggests that the relaxation processes in PMMA will have a very limited direct influence on the total dielectric response for the polymer gels. The polymer will, however, indirectly affect the data by dynamical coupling to relaxation of PC molecules.

To accurately separate the response from PC and PMMA an effective medium analysis is required. Such analysis requires information about the nanoscopic structure of the system, which is presently not available for our system. However, the connectivity of the polymer chains together with percolation theory yields that both the PC and PMMA must be continuous phases for the investigated samples. For such a system, Pelster[22] has performed an approximate effective medium analysis that demonstrated that the intrinsic peak position of the solvent is not altered compared to the experimentally measured effective position. In his analysis the shape of the relaxation function also remains practically unaffected, while the amplitude of the response has an almost linear dependence on the relative amount of solvent compared to the polymer. All major features of the effective response can thus be directly coupled to the intrinsic relaxation of the PC in our system. The loss peak attributed to the α

relaxation of PC becomes smaller, broader, and slower with decreasing PC concentration as seen in Fig. 2. With PC concentration levels below 30% the loss peak becomes so small that the possibility of contributions from polymer relaxation processes no longer can be ignored. Therefore we only discuss data obtained for PC concentrations larger than 30% in this paper.

The α relaxation can, under the present experimental condition, only be observed up to 182 K for systems with a high content of PC. This is due to crystallization of PC, which is directly observed in the dielectric spectra as a significant decrease in the amplitude of the loss peak. These observations are consistent with those reported by Schneider *et al.*[31] for bulk PC where they note a high probability of crystallization especially around 180 K. Even after crystallization has occurred a small loss peak can be detected, although the shape is very different compared to that observed before crystallization. This suggests that a small amount of PC remains in an amorphous state. Data obtained after partial crystallization are not considered in this paper. For polymer gels with a PC concentration less than 75% no crystallization was detected.

To analyze the dielectric loss peak in more detail we use a recently proposed empirical function[32]

$$\varepsilon''(\omega)=\frac{\varepsilon_p''}{\dfrac{1-|a-b|}{a+b}\left[b(\omega/\omega_p)^{-a}+a(\omega/\omega_p)^{b}\right]+|a-b|}, \tag{2}$$

where ω_p is the peak position and $0<a,b\leqslant 1$ are shape parameters. A sum of a low-frequency power law ($\varepsilon''\propto\omega^{-s}$, $0\leqslant s\leqslant 1$) and Eq. (2) were fitted to the imaginary part of the permittivity obtained from the experiments. The curve fits were performed with a linear weighting over a logarithmic frequency range such that the influence of the loss peak is roughly equal to that of the power-law and the high-frequency excess wing[33] was excluded. The reason for choosing Eq. (2) is our focus on the limiting power-law behavior above and below the peak frequency for which Eq. (2) is a convenient tool. Equation (2) is derived from the assumption of power-law behaviors below $[\varepsilon''(\omega)\propto\omega^{a}]$ and above $[\varepsilon''(\omega)\propto\omega^{-b}]$, a loss peak at the peak frequency ω_p with the amplitude ε_p''. We note that a Fourier-transformed KWW expression [Eq. (1)] is well approximated by Eq. (2) with $a=1$ and $b\approx\beta_{\mathrm{KWW}}$.[32] We also note that the data can be described by the Havriliak-Negami (HN) function, but that the HN function consistently gives mean-square deviations that are at least a factor 2 larger than those obtained when using Eq. (2). Similarities and differences between some of the most commonly used functions to describe dielectric loss peaks, including the HN function and Eq. (2) are discussed in detail in Refs. 32 and 34.

In Fig. 3 we show an example of the total curve fit to data, including the loss peak and the low-frequency dispersion. From this procedure we extract the temperature and concentration dependencies of the relevant dynamical parameters. Also note the appearance of the excess wing at the highest frequency (see Ref. 33), which is excluded from the scope of this paper. In Fig. 4 the most probable relaxation time, $\tau=2\pi/\omega_p$, is plotted versus the inverse temperature for the different PC concentrations. As seen in the graph, starting with pure PC and increasing the amount of PMMA results in a gradual shift of the relaxation time to longer time scales. It is also seen that the temperature dependence of the relaxation time distinctly deviates from an Arrhenius behavior for all the investigated samples.

The gradual increase of the relaxation time as the glass transition temperature is approached is commonly described by the Vogel-Fulcher-Tammann (VFT) expression[23,35]

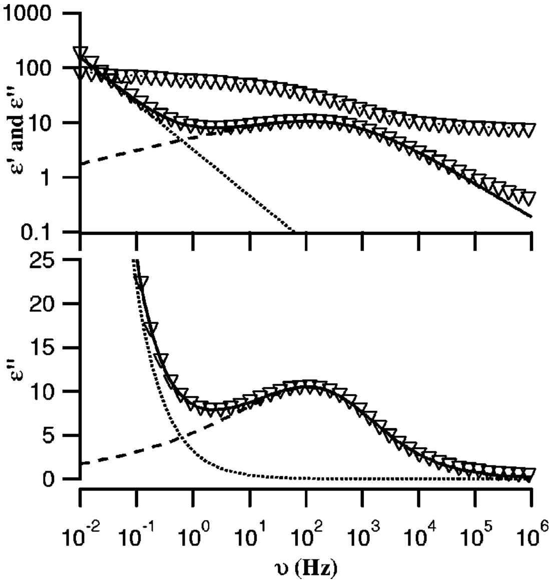

FIG. 3. Experimental data for a polymer gel consisting of 75% PC and 25% PMMA, together with the obtained result from the curve fit to Eq. (2). The upper part shows the real (triangles with dots) and imaginary (triangles) parts of the permittivity on a logarithmic scale. The lower part shows the imaginary part of the permittivity on a linear scale. Note that the excess wing is not included in the curve-fit range.

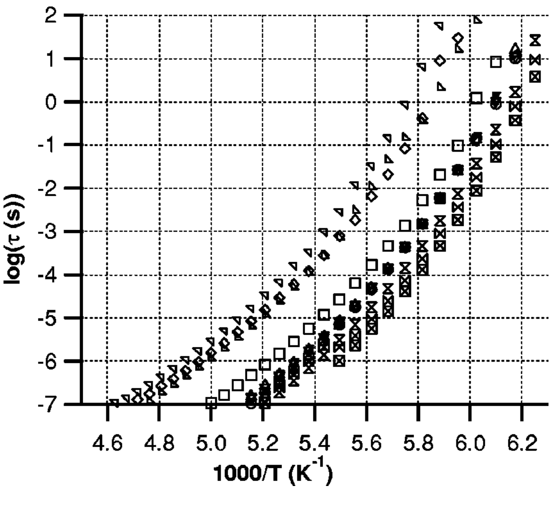

FIG. 4. Arrhenius plot of the relaxation time τ, as obtained form curve fitting to Eq. (2) plotted versus inverse temperature. The symbols representing the different samples are shown in Table I.

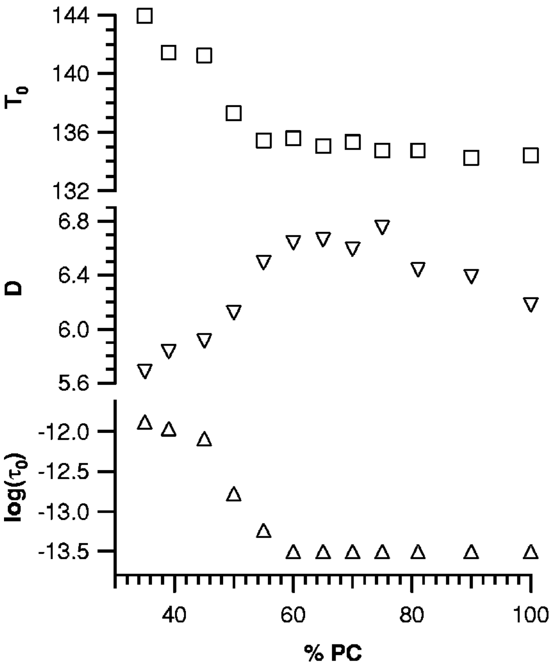

FIG. 5. VFT parameters (a) τ_0, (b) D, and (c) T_0, as a function of PC concentration.

$$\tau = \tau_0 \exp\left[\frac{DT_0}{T-T_0}\right]. \tag{3}$$

where T_0 is the temperature where τ diverges and D describes the deviation from an Arrhenius behavior. For all the investigated samples in our study the temperature dependence of the relaxation time can satisfactorily be described by the VFT expression. The obtained VFT parameters are given in Table I and also shown in Fig. 5 as a function of PC concentration. Generally, the most dramatic changes for all the VFT parameters occur for PC concentrations below 60%. No systematic changes of τ_0 from the value obtained for pure PC could be detected down to 60% PC. Since the curve-fit parameters are highly interdependent the value of τ_0 was kept fixed to the value for bulk PC over the range 60%–100% PC to ensure stable fits. Below 60%, τ_0 and T_0 systematically become larger with decreasing PC concentration. The value of D, on the other hand, tends to be even larger than bulk PC for intermediate concentrations PC (~70% PC) but lower than bulk PC for concentrations below 50%.

The shape of the loss peak is determined by the a and b parameters [Eq. (2)], which are plotted as a function of temperature and concentration in Fig. 6. From the graph we can make some observations which are common for both shape parameters. First, both a and b decrease with increasing polymer content and secondly, both increase with increasing temperature. However, the detailed behavior is different for the high- and low-frequency exponents, which will be discussed in more detail below.

For bulk glass formers there is generally a strong correlation between the b parameter, and the fragility parameter D, as discussed by Böhmer *et al.*[24] However, bulk PC is a distinct exception from this behavior, being a very fragile glass former, yet with a rather narrow loss peak.[24] In this context it is interesting to note that the fragility parameter D is almost independent of the PC concentration (see Fig. 5) despite the decrease in b (see Fig. 6).

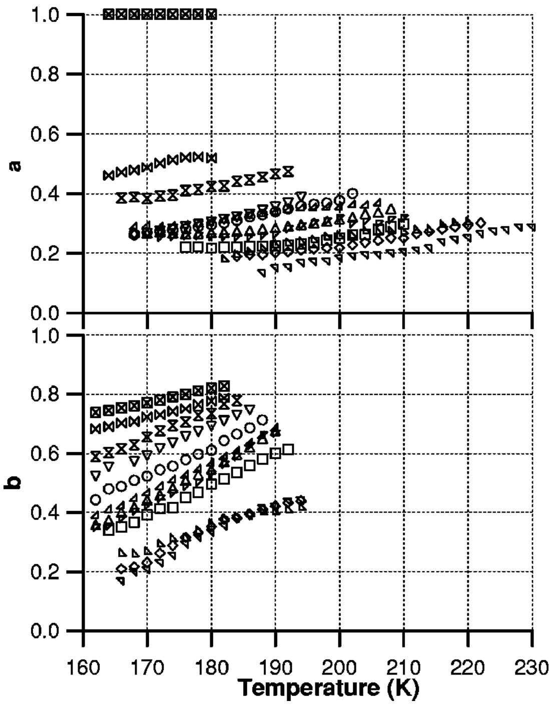

FIG. 6. Shape parameters a and b of Eq. (2) as a function of temperature and PC concentration. The symbols representing the different samples are given in Table I.

IV. DISCUSSION

A. Confinement effects on the PC dynamics

The focus of this study is the effects of the α relaxation when PC is restricted to move in a polymer matrix. To correctly describe the loss peak the low-frequency dispersion has to be properly accounted for. The low-frequency dispersion has a behavior that cannot be explained by normal conductivity since the imaginary part of the permittivity is not inversely proportional to the frequency.[12] One plausible explanation for this behavior is Maxwell-Wagner relaxation, which is commonly observed for composite materials.[12,39] This attribution is supported by the observation that for some of the samples a ‘‘shoulder’’ appears at very low frequencies. The observed behavior is rather similar to that reported by Arndt *et al.* for salol confined in porous glass.[12] An alternative explanation is polarization of domains according to the model proposed by Jonscher.[40] The gel system fulfills the basic assumptions of the Jonscher model with PC-rich domains separated by the polymer network or, alternatively, domains with high polymer concentration. An additional complication for a definite attribution of this decay is the possibility of polymer relaxation, or PC molecules in close proximity to a polymer chain, which may contribute to the dielectric response in this low-frequency region. Thus, there are many possible explanations for the observed low-frequency behavior, which makes a definite attribution difficult.

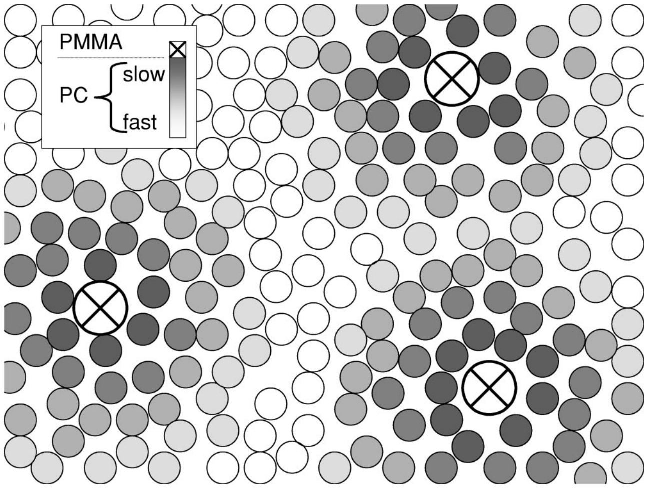

FIG. 7. Schematic two-dimensional picture of our simple model used to describe the dynamics. The circles with crosses symbolize the polymer chain. Circles without crosses represent the solvent molecules and the darker color the slower motion.

For the loss peak attributed to the α relaxation of PC we observe a slowing down and broadening of the peak with increasing polymer content. An appealing idea is to attribute the broadening to a more heterogeneous dynamical surrounding of the PC molecules with increasing polymer content. This idea qualitatively explains the data if we assume that a PC molecule in close proximity to a slower polymer chain is restricted in motion. Similar ideas have previously been used to interpret experimental data for other polymer/solvent systems (see Ref. 41, and references therein). A schematic picture visualizing this basic idea is shown in Fig. 7. The assumption in our model can also be formulated to be that the confinement effects are mainly due to surface effects, and finite-size effects are only indirectly observable as discussed below. The surface in our gel system is visualized as the interface between the polymer chains and the solvent, i.e., tubes around the polymer. One important feature is the dimensionality of the spatial restrictions of the PC molecules; in our gel system they are able to move in three dimensions and only restricted by practically one-dimensional polymer chains. Furthermore, the restricting polymer chains are not perfectly static since they are dissolved in PC. The dynamics of the polymer chains is not directly detectable in the present experiments due to the smaller dielectric constant for PMMA compared to that for PC. However, for other polymer/solvent combinations the polymer has been shown to be much slower than the solvent[41,42] and in the present system the presence of cross links in the gel can further decrease the dynamics of the polymer. In addition to segmental relaxations of the backbone, PMMA has secondary relaxations, which is normally attributed to more localized side-chain dynamics.[25] Such secondary processes may be important for the dynamical coupling between the solvent and the polymer and thus of importance for the degree of spatial restriction imposed by the polymer on the solvent. The investigated gel system therefore provides a different confinement geometry than, for example, porous glasses or layered structures. Nonetheless, the concepts frequently used when discussing other more common confinements are applicable also for our system and thus we consider our gel system as an alternative confinement geometry.

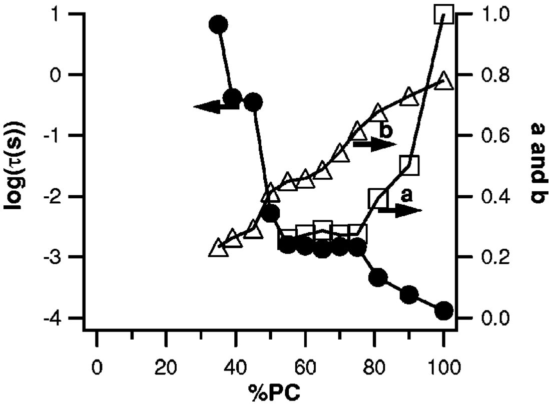

FIG. 8. The relaxation time (filled circles) and shape parameters a (squares) and b (triangles) at $T=172$ K for different PC concentrations. The errors obtained from the least-squares fits are of the size of the symbols.

For the dynamical behavior of our gel system the interaction between PC and PMMA is important, which is not known in detail. Previous Raman-scattering experiments exclude strong interactions between PMMA and PC.[36] We also note that PC is a good solvent for PMMA,[37] and that they are miscible in all tested concentrations. This suggests that the chemical interaction between PC and PMMA is weak. This in turns implies that the influence of the polymer is mainly caused by spatial restrictions and not due to strong chemical interaction between the polymer and PC molecules. Our assumption of a layer of slower PC dynamics around the polymer is consistent with experiments on PC confined in porous glass, which show a slower relaxation process unless special precautions are taken to reduce the surface interaction.[12,13] Also molecular-dynamics simulations of Lennard-Jones materials show such behavior.[38]

To examine the correlation between the relaxation time and the shape of the relaxation we show the shape parameters a and b together with $\log(\tau)$ at $T=172$ K for all examined PC concentrations in Fig. 8. One important difference between bulk and confined PC is the broadening also at the low-frequency side quantified by the a parameter, which possibly is due to the heterogeneity induced by the polymer giving a wider distribution of relaxation times. The transition from bulk to confined behavior is gradual but not uniform. One region with markedly increasing relaxation times upon decreasing PC concentration is the range from 90% down to 75% PC. This is also the region where the crystallization of PC ceases to occur. These changes are accompanied by a pronounced increase in the macroscopic viscosity as tested by a flow experiment and may be interpreted as a transition from a polymer in solution state to a gel state. The a parameter shows dramatic changes within this low polymer concentration region. This parameter is controlled by slow motions and thus mainly comparatively large length scale relaxations. The data therefore suggests that the main change in the dynamics in this region (75%–90% PC) is a slowing down of relaxation processes over large length scales. The influence of the polymer matrix may then be regarded as a loose network with significantly lower mobility, at least at larger length scales, than the solvent. We also note that this behavior is obtained for relatively moderate polymer concentration after which further increase in the polymer concentration only weakly affects the *a* parameter. The experimentally observed $a<1$ also infers that a Fourier-transformed KWW expression will not accurately describe the data as discussed in Ref. 32.

After the initial slowing down of the dynamics a plateau with less concentration dependence is observed. In this region, from 75% down to 55% PC, both the low-frequency parameter *a* and the relaxation time are almost independent of the PC concentration. Since the relaxation time is only about one order-of-magnitude slower than bulk PC it suggests that despite the huge difference in macroscopic viscosity the microscopic dynamics still have some resemblance to that of the pure PC. We note the remarkably high correlation between the relaxation time and the shape parameter *a* over the PC concentration range from 100% down to 55%.

Previous dynamic light-scattering experiments[43,44] performed on similar systems showed a complex relaxation behavior, which was attributed to a diffusive motion of PC and to segmental relaxation of the polymer matrix. The results showed that the diffusive motion of the solvent becomes drastically slower as the polymer concentration approaches 50%.[44] Interestingly, we observe a similar behavior in the present study, which can be seen in Fig. 4. Moreover, T_0 in Eq. (3) (see Fig. 5) also shows a marked increase as the PC concentration is decreased below roughly 50%. The similarities occur despite the fact that the light-scattering experiment probes dynamics of length scales roughly 1000 times larger than a typical dipole-dipole distance in our system, which is an estimate of the length scale probed by dielectric spectroscopy.[26] Further information about the origin of this feature can be obtained from examining the *b* parameter since this also decreases in this region (see also Fig. 6). The high-frequency parameter *b* is determined by rather localized processes and should therefore reflect the dynamical coupling between mobile PC molecules and their neighbors. The observed threshold around 50% may then be interpreted as the concentration for which practically all solvent molecules become affected by the presence of the polymer chains and where the remaining liquidlike properties vanish at a local level. Beyond this threshold it is probably more correct to consider the system as a plasticized polymer.

B. Cooperative dynamics

We now focus our attention on the temperature and concentration dependencies of the relaxation strength and how they may be used to monitor the cooperative dynamics. From the present experimental data it is difficult to extract the relaxation strength $\Delta\varepsilon=\varepsilon_s'-\varepsilon_\infty'$ directly from the real part of the permittivity since the low-frequency dispersion obscures a direct determination. Our approach has instead been to use the parameters obtained from the curve fit of Eq. (2) in order to numerically calculate the corresponding real part using the Kramers-Kronig relation. This procedure gives a relaxation strength exclusively determined by the observed loss peak, which we attribute to the modified α relaxation of the PC molecules as discussed above. In Fig. 9 $\Delta\varepsilon(T)/\Delta\varepsilon(T_g)$ is shown, i.e., the relaxation strength normalized by the relaxation strength at $T_g=T$ $(\tau=100\ \mathrm{s})$, for each sample. For bulk PC a small decrease with increasing temperature is observed in agreement with the literature.[31] Also for samples with only a low concentration of polymer a very weak temperature dependence is observed. This is in clear contrast to the marked increase of the relaxation strength observed for the polymer gel in the range 50%–65% PC. The relaxation strength is to a large extent determined by the dipole moment of the molecules and the number density of particles participating in the processes. The latter explains the observed decrease in the amplitude with decreasing PC concentration. This implies, at least to a first approximation, that the number of molecules participating in the observed relaxation process in bulk PC is practically temperature independent. However, for samples with a high polymer content the number of participating molecules is strongly temperature dependent.

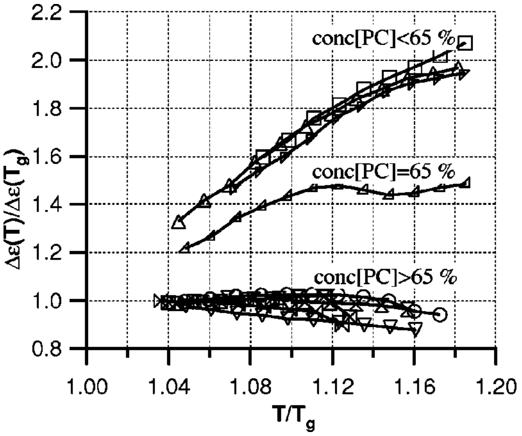

FIG. 9. Relaxation strength normalized with the relaxation strength at T_g as a function of temperature from 156 to 180 K for different PC concentrations. Table I shows the symbols used for the different samples.

To explain our experimental data shown in Fig. 9 we return to the simple model of the dynamics introduced above (see also Fig. 7) and combine it with the concept of cooperativity. We envision that PC molecules within a certain distance, determined by the cooperative dynamics of PC, from a polymer chain, will be influenced by the much slower dynamics of the polymer. At temperatures close to T_g the cooperativity regions are assumed to be large. The fraction of PC molecules that are significantly slowed down by the proximity to the polymer and shifted out of our experimental frequency range will then be large at low temperatures. Upon increasing the temperature the cooperativity length decreases and the volume around each polymer chain with PC molecules experiencing slower dynamics will decrease, i.e., more PC molecules relax via the observed α relaxation. Thus in our model the relaxation strength for PC molecules in the confined systems will increase with increasing temperature, which is consistent with our experimental observations (see Fig. 9).

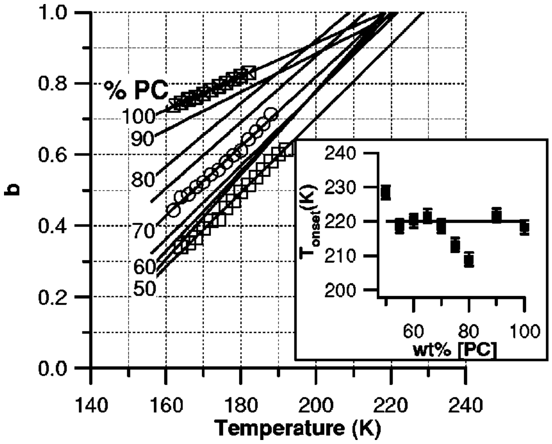

FIG. 10. Temperature dependence of the high-frequency power-law exponent *b*, with the extrapolation included. The inset shows the onset temperature T_{onset}, as a function of weight percent PC.

C. Temperature dependence of the size of cooperative regions

An interesting observation is the almost perfectly linear temperature dependence obtained for the *b* parameter within the observable experimental range, see Fig. 6. Extrapolating this linear behavior to *b* equals unity, i.e., a high-frequency slope identical to the simple Debye case gives a rough estimate of an onset temperature for cooperativity. The interesting new feature in this study is that we observe that T_{onset} obtained from an extrapolation of the low-temperature values is remarkably independent of the polymer concentration. It is observed in a narrow temperature range $T_{\mathrm{onset}}=220\pm 2$ K, as seen in the inset in Fig. 10, with slight exceptions for the samples with 75% and 80% PC and <50% PC. It should be noted that different absolute values and a different temperature dependence of the high-frequency power-law exponent is obtained if, for example, the Havriliak-Negami expression is used instead of Eq. (2). However, a number of arguments is in favor of our choice of data analysis procedure compared to the use of the HN expression: (i) the high-frequency power-law exponent is obtained directly from one curve-fit parameter, (ii) with $a=1$, Eq. (2) is a good approximation to a Fourier transform of the KWW expression, and (iii) Eq. (2) gives smaller mean-square deviations with the same number of curve fit parameters and has a smoother temperature dependence.[34]

Extending our analysis we can also use the *b* parameter to estimate the temperature dependence of the size of cooperative regions. At temperatures slightly below the onset temperature, cooperativity arguments give that the dynamics should hardly be affected by the PMMA matrix since for any given PC molecule, there will always be at least one neighboring PC molecule in all samples with a moderate concentration of PMMA. However, lowering the temperature leads to larger cooperativity regions and the confinement effects thus become more pronounced the higher the polymer concentration. This implies that we expect to see larger temperature dependence for the shape of the relaxation function with higher polymer concentration, which indeed is seen in the larger temperature dependence on *b* (see Fig. 6). This reasoning eventually breaks down when the polymer content becomes too high and this is indeed experimentally observed for samples with <50% PC, which appears to be a threshold concentration as, for example, seen for T_0 in Fig. 5. The somewhat lower T_{onset} for samples with 75% and 80% PC clearly demands further studies. Here we only note that these relatively small deviations coincide with large changes in both the macroscopic viscosity and the relaxation time. However, it is important to point out that both above and below this concentration range our data give the same T_{onset} within experimental uncertainty (see inset in Fig. 10) implying a similar physical origin. It has also to be emphasized that the analysis is based on experimental results obtained only up to roughly 192 K and that the excess wing is excluded. The proposed merging at 220 K is therefore based on the extrapolations of the linear behavior observed in the experimental temperature range. Schneider *et al.*[31] reported a β_{KWW} for bulk PC that levels off below unity in contrast to the results obtained by Schönhals *et al.*,[29] where β_{KWW} indeed does approach unity at a temperature $T_A=217$ K, in excellent agreement with our results. We note that the α relaxation for confined systems does not necessarily become a Debye-type relaxation at the observed onset temperature since the low-frequency shape parameter [a in Eq. (2)] may still be less than unity at this temperature.

It is also interesting to see how our cooperativity related temperature compares with other transition temperatures for PC. First we note the intriguing match between $T_{\mathrm{onset}}=220\pm 2$ K and the melting temperature of bulk PC, $T_m=218$ K. Whether the crystallization temperature is connected to the cooperativity behavior, and if this connection is general demands further studies. We note that T_{onset} is almost constant despite the absence of any detectable crystallization (within our experimental temperature range) for samples with PC concentrations less than 80%. This raises a second important question: is there a connection between the thermodynamically controlled crystallization process and cooperative dynamics also in systems which cannot crystallize *macroscopically*? Kivelson *et al.*[45,46] have previously suggested that the onset temperature for cooperativity, by them denoted T^*, is always larger than or equal to the melting temperature, $T^* \geqslant T_m$. Their model also predicts a transition from Arrhenius to "super-Arrhenius" temperature dependence of the relaxation time at T^*. For bulk PC, dielectric spectroscopy yields $T^*=215$ K,[31] while $T^*=235$ K has been obtained from other techniques.[45,46] As mentioned above, Schönhals *et al.*[29] use a slightly different approach and report a transition between an Arrhenius temperature dependence and a VFT region for bulk PC at a temperature $T_A=217$ K, which matches our T_{onset}. This strengthens the identification of the transition temperature to the onset of cooperativity.

V. CONCLUSIONS

We have studied the α relaxation of PC restricted to move in a polymer matrix. Our results from dielectric spectroscopy show that the α relaxation becomes slower and broader with increasing polymer concentration. These features are due to the gradual increase of the influence of added polymer, which increases the structural heterogeneity of the system. The limiting power-law behaviors and thus the broadening of the loss peak are dependent on both temperature and PC concentration. The coincidence of large changes at the low-frequency side of the loss peak with an increase in the relaxation time in the region from 90% down to 75% PC is attributed to spatial restriction imposed by the polymer on long-range PC motion. The high-frequency side, i.e., more localized processes, is mostly affected in the range from 55% down to 45% PC where a dramatic increase of the relaxation time occurs. These features are attributed to the increasing importance of the interaction between the polymer and solvent dynamics and the gradual decrease of PC molecules that are unaffected by the polymer. We also discussed the dynamics in terms of cooperativity effects.

The present study shows that investigations of polymer gels can provide complementary information to other confinement experiments such as those performed using porous glasses. The advantage of being able to systematically increase or decrease the amount of restricting polymer opens new routes to understanding some of the fundamental aspects of the glass transition. Of specific interest is the length scale dependence of the dynamics in the supercooled regime. The overall picture of solvent dynamics that emerges from our findings is that at high frequencies the properties remain liquidlike even with a substantial amount of polymer. The low-frequency slope is more directly affected by the presence of the polymer and has a close relation to the macroscopic viscosity. Of special importance is the decoupling between the macroscopic viscosity and the molecular motions which exist to a large extent in polymer gels. We also hope that in the future we will be able to combine the dynamical results presented here with structural information.

ACKNOWLEDGMENTS

Financial support from the Swedish Natural Science Research Council and the Swedish Foundation for Strategic Research is gratefully acknowledged.

---

*Author to whom correspondence should be addressed. Email address: svanberg@fy.chalmers.se

[1] P.-G. de Gennes, *Scaling Concepts in Polymer Physics* (Cornell University, Ithaca, 1979).

[2] M. Doi and S. F. Edwards, *The Theory of Polymer Dynamics* (Oxford Science Publications, Oxford, 1986).

[3] G. Adam and J. Gibbs, J. Chem. Phys. **43**, 139 (1965).

[4] D. Sappelt and J. Jäckle, J. Phys. A **26**, 7325 (1993).

[5] A. Hunt, Solid State Commun. **90**, 527 (1994).

[6] H. Huth, M. Beiner, and E. Donth, Phys. Rev. B **61**, 15 092 (2000).

[7] R. Richert, Phys. Rev. B **54**, 15 762 (1996).

[8] G. Barut, P. Pissis, R. Pelster, and G. Nimtz, Phys. Rev. Lett. **80**, 3543 (1998).

[9] D. Daoukaki, G. Barut, R. Pelster, G. Nimits, A. Kyritsis, and P. Pissis, Phys. Rev. B **58**, 5336 (1998).

[10] A. K. Rizos and K. L. Ngai, Phys. Rev. E **59**, 612 (1999).

[11] E. Donth, J. Polym. Sci., Part B: Polym. Phys. **34**, 2881 (1996).

[12] M. Arndt, R. Stannarius, W. Gorbatschow, and F. Kremer, Phys. Rev. E **54**, 5377 (1996).

[13] M. Arndt, R. Stannarius, H. Groothues, E. Hempel, and F. Kremer, Phys. Rev. Lett. **79**, 2077 (1997).

[14] C. L. Jackson and G. B. McKenna, J. Non-Cryst. Solids **131-133**, 221 (1991).

[15] J. Schuller, Y. B. Mel'nichenko, R. Richert, and E. W. Fischer, Phys. Rev. Lett. **73**, 2224 (1994).

[16] J. Schuller, R. Richert, and E. W. Fischer, Phys. Rev. B **52**, 15 232 (1995).

[17] H. Wendt and R. Richert, J. Phys.: Condens. Matter **11**, A199 (1999).

[18] P. Pissis, A. Kyritsis, D. Daoukaki, G. Barut, R. Pelster, and G. Nimitz, J. Phys.: Condens. Matter **10**, 6205 (1998).

[19] C. Donati and J. Jäckle, J. Phys.: Condens. Matter **16**, 2733 (1996).

[20] C. Bennemann, C. Donati, J. Baschnagel, and S. C. Glotzer, Nature (London) **399**, 246 (1999).

[21] M. Russina, F. Mezei, R. Lechner, S. Longeville, and B. Urban, Phys. Rev. Lett. **84**, 3630 (2000).

[22] R. Pelster, Phys. Rev. B **59**, 9214 (1999).

[23] C. A. Angell, Science **267**, 1924 (1995).

[24] R. Böhmer, K. L. Ngai, C. A. Angell, and D. J. Plazek, J. Chem. Phys. **99**, 4201 (1993).

[25] N. G. McCrum, B. E. Read, and G. Willliams, *Anelastic and Dielectric Effects in Polymer Solids* (Wiley, New York, 1967).

[26] R. Bergman, F. Alvarez, A. Alegria, and J. Colmenero, J. Chem. Phys. **109**, 7546 (1998).

[27] H. Sillescu, J. Non-Cryst. Solids **243**, 81 (1999).

[28] H. Wendt and R. Richert, Phys. Rev. E **61**, 1722 (2000).

[29] A. Schönhals, F. Kremer, A. Hofmann, E. W. Fischer, and E. Schlosser, Phys. Rev. Lett. **70**, 3459 (1993).

[30] C. Svanberg, W. Pyckhout-Hintzen, and L. Börjesson (unpublished).

[31] U. Schneider, P. Lunkenheimer, R. Brand, and A. Loidl, Phys. Rev. E **59**, 6924 (1999).

[32] R. Bergman, J. Appl. Phys. **88**, 1356 (2000).

[33] U. Schneider, R. Brand, P. Lunkenheimer, and A. Loidl, Phys. Rev. Lett. **84**, 5560 (2000).

[34] C. Svanberg and R. Bergman, Philos. Mag. B **82**, 517 (2002).

[35] M. D. Ediger, C. A. Angell, and S. R. Nagel, J. Phys. Chem. **100**, 13 200 (1996).

[36] D. Ostrovskii, A. Brodin, L. M. Torell, G. B. Appetecchi, and B. Scrosati, J. Chem. Phys. **109**, 7618 (1998).

[37] *Polymer Handbook*, edited by J. Brandrup and E. H. Imergut (Wiley-Interscience, New York, 1989).

[38] P. Scheidler, W. Kob, and K. Binder, J. Phys. IV **10**, 33 (2000).

[39] K. W. Wagner, Arch. Elektrotech. (Berlin) **2**, 378 (1914).

[40] A. K. Jonscher, J. Phys. D **32**, R57 (1999).

[41] G. Floudas, G. Fytas, and W. Brown, J. Chem. Phys. **3**, 2164 (1996).

[42] K. Adachi and T. Kotaka, Polym. J. (Tokyo) **13**, 687 (1981).

[43] C. Svanberg, J. Adebahr, H. Ericson, L. Börjesson, L. M. Torell, and B. Scrosati, J. Chem. Phys. **111**, 11 216 (1999).

[44] C. Svanberg, J. Adebahr, R. Bergman, L. Börjesson, B. Scrosati, and P. Jacobsson, Solid State Ionics **136-137**, 1147 (2000).

[45] D. Kivelson, S. A. Kivelson, X. Zhao, Z. Nussinov, and G. Tarjus, Physica A **219**, 27 (1995).

[46] D. Kivelson, G. Tarjus, X. Zhao, and S. Kivelson, Phys. Rev. E **53**, 751 (1996).